SCIENCE CHINA
Chemistry

• REVIEWS •
• SPECIAL TOPIC • New Researches of State Key Laboratories in Analytical Chemistry

July 2016 Vol. 59 No.7: 783–793
doi: 10.1007/s11426-016-5570-7

Recent progress in gold nanoparticle-based biosensing and cellular imaging

Haiyang Peng, Hao Tang* & Jianhui Jiang*

State Key Laboratory of Chemo/Bio-Sensing and Chemometrics; College of Chemistry and Chemical Engineering, Hunan University, Changsha 410082, China

Received November 28, 2015; accepted December 21, 2015; published online March 16, 2016

Gold nanoparticles (AuNPs) have been extensively used in optical biosensing and bioimaging due to the unique optical properties. Biological applications including biosensing and cellular imaging based on optical properties of AuNPs will be reviewed in the paper. The content will focus on detection principles, advantages and challenges of these approaches as well as recent advances in this field.

gold nanoparticle, optical, functionalization, biosensing, cellular imaging

Citation: Peng HY, Tang H, Jiang JH. Recent progress in gold nanoparticle based biosensing and cellular imaging. *Sci China Chem*, 2016, 59: 783−793, doi: 10.1007/s11426-016-5570-7

1 Introduction

Biosensors represent a promising tool to achieve the rapid, sensitive, and selective analysis of molecules of interest for clinic diagnosis, environmental monitoring, and many other applications [1]. With the advances in nanotechnology, nanomaterials have been utilized in biosensing approaches due to its unique physicochemical properties, such as high surface-to-volume ratio, enhanced optical properties, and excellent electrical properties [2,3]. All these features are favorable for the recognition and transduction processes of biosensors, which enable the improvements in selectivity, response time, signal-to-noise (*S*/*N*) ratio, and limits of detection (LOD).

Gold nanoparticles (AuNPs) possess distinct physical and chemical properties, which make them appropriate fabrication materials of novel biosensors. The synthesis methods of AuNPs enable the preparation of AuNPs in controllable sizes and shapes and realize tunable physicochemical and surface properties. AuNPs have unique optical properties due to the surface plasmon resonance and the surface of AuNPs can be easily functionalized with different molecules for molecular recognition. Moreover, AuNPs are stable, biocompatible, and slightly toxic to cells and can easily enter cells. All these favorable features make AuNPs an attractive option for bioprobes and bioimaging applications. Several reviews regarding biological applications of AuNPs have been published in the past five years [4–7]. These review articles focused on the comprehensive introduction of biological applications of AuNPs or specific topic such as the uptake of AuNPs into cells. In this paper, we will discuss the biological applications based on optical properties of AuNPs (Figure 1). Biosensing strategies *in vitro* utilizing light absorption, fluorescence and surface enhanced Raman spectroscopy (SERS) of AuNPs will be included. The content will focus on detection principles, advantages and challenges of these approaches and recent advances will be highlighted. Cellular imaging approaches utilizing fluorescence, light scattering, and two-photon photoluminescence

*Corresponding authors (email: haotang@hnu.edu.cn; jianhuijiang@hnu.edu.cn)

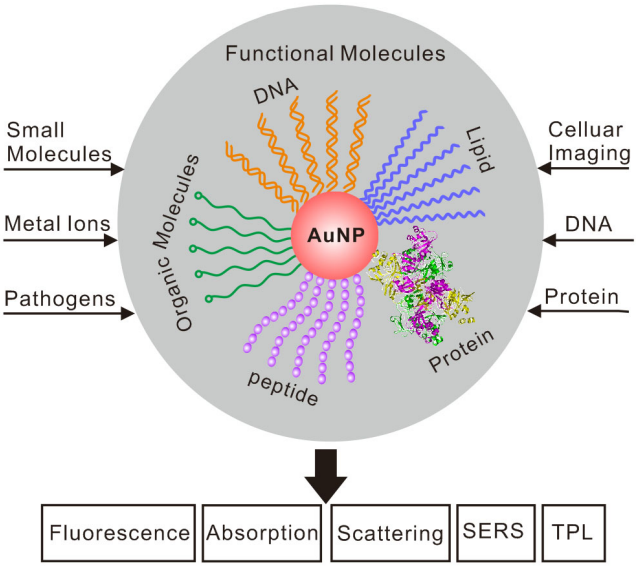

Figure 1 Schematic illustration of functionalized AuNPs for different optical biosensing and bioimaging applications (color online).

of AuNPs will be discussed.

2 Optical properties of AuNPs

AuNPs own unique optical properties due to the surface plasmon resonance, which makes them useful for biosensing *in vitro* and *in vivo*. The surface plasmon resonance highly depends on the sizes and shapes of AuNPs, and is sensitive to the local medium of AuNPs surface [8–12]. The changes in the surroundings (surface charge, aggregation state, etc.) will lead to the changes in surface plasmon frequency and can be utilized in biosensing approaches. The absorption and scattering of incident light of AuNPs are greatly enhanced due to the surface plasmon resonance. Absorption and scattering of AuNPs are 4–6 orders of magnitude stronger than absorption of organic dyes and the emission of strongly fluorescent molecules, respectively [10]. Hence, biosensors can be developed based on plasmon absorption changes with a decent sensitivity. Owing to the strong absorption, AuNP is an effective quencher for various fluorophores and fluorescence-based biosensor can be devised. It is worth noting that gold nanoparticle is an effective SERS substrate for developing SERS-based biosensors due to the surface plasmon resonance.

Optical properties and biosensing application of gold nanospheres and gold nanorod structures are mostly widely studied, and other structures such as core-shell, cube, cage and star have also been used in biosensing and bioimaging [13–18]. The surface plasmon band of gold nanosphere particles is at 520 nm in the visible range and varies with the particle size. Gold nanorods have been widely applied in biosensing and bioimaging because this anisotropic shape usually displays two different plasmon bands: one band in the visible range corresponds to the short axis; the other in visible or near-infrared range corresponds to the long axis. The two plasmon bands are tunable by controlling the dimension of the nanorods, thus making gold nanorods attractive for optical application. Moreover, these anisotropic gold nanorods may have different reactivities for different crystal faces and can be used for controllable assembly.

3 Synthesis and surface functionalization of gold nanoparticles

Various kinds of methods for synthesis of AuNPs have been developed [14, 19–24]. In general, the simplest way of synthesizing AuNPs is to reduce chloroauric acid in aqueous phase. A classic preparation method of colloidal stable AuNPs is to use citrate as reducing and capping agent. After nucleation, citric acid can be adsorbed on AuNPs to provide colloidal stability due to the negative charges. Gold nanosphere particles are obtained because spheres are the shape with the lowest energy. The size of spherical citrate-capped AuNPs can be tuned from 15 to 150 nm based on different reaction conditions. To prepare AuNPs with different shapes and structures, mild reducing agents and surfactants or templates are often required. Seeded growth is a common way to control the shapes of gold nanoparticles, such as gold nanorods, triangles, cubes, and stars [14].

The surface of the synthesized AuNPs is surrounded by different stabilizing molecules to provide stability and prevent aggregation according to different synthesis routes. However, for the purposes of biosensing and bioimaging, surface functionalization should be performed to improve biocompatibility, reduce toxicity, and coat AuNPs with molecular probes. Various surfactants or biomolecules can be used to replace the original ligand and then introduce different functional moieties for biosensing and bioimaging [25, 26]. A common method for AuNPs functionalization is to introduce thiol group via ligand exchange reaction because thiol group can react with gold surfaces to form stable Au:S bond [27]. Thiolated ligand is useful for the introduction of target moieties and different functional molecules for AuNPs. For example, Mikin's group [28, 29] developed the spherical nucleic acid (SNA) construct with oligonucleotide functionalized AuNPs. High-density oligonucleotides can be assembled on the surface of AuNPs via Au:S bond by means of initial DNA adsorption and salt aging processes (Figure 2). The SNA construct is stable under different ionic strength conditions. High local sodium ion concentration around the oligonucleotide enables deactivation of many nucleases and prevents the cleavage of DNA probes [30]. All these features make SNA useful for biosensing and bioimaging applications [31–35].

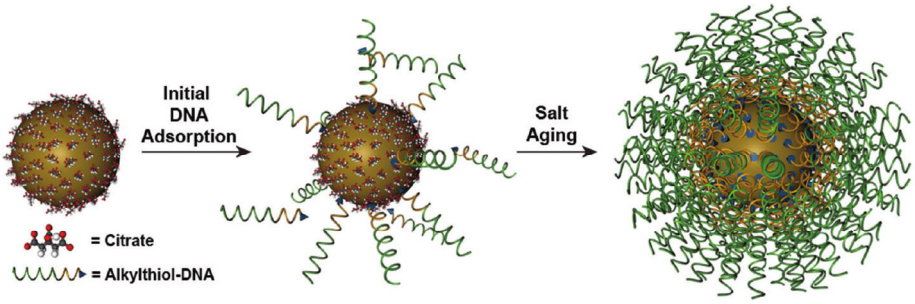

Figure 2 Preparation of high-density oligonucleotides functionalized core-shell SNA construct with alkylthiol-functionalized oligonucleotides via Au:S bond. Reproduced with permission from Ref. [29]. Copyright 2012, American Chemical Society (color online).

4 AuNPs-based biosensing *in vitro*

The ever increasing demand of *in vitro* detection for clinic diagnostics and environmental monitoring requires cheap, rapid, sensitive, and portable assay approaches. AuNPs-based optical in vitro biosensing approaches have gained wide attention due to the excellent optical properties including: enhanced surface plasmon absorption, strong fluorescence photoluminescence and fluorescence quenching ability, and SERS. These properties make AuNPs excellent candidates for the development of biosensors for various targets. In the past several years, AuNPs-based optical biosensing *in vitro* provided many innovative approaches for the detection of a series of target analytes such as metal ions, proteins, nucleic acids, and small molecules in a rapid and efficient manner.

4.1 AuNPs-based colorimetric assay

The AuNPs-based colorimetric assay has drawn wide attention since the signal readout is based on color change and can be recorded with a cheap spectrometer or even naked eye. The surface plasmon resonance frequency of AuNPs is sensitive to the surrounding of the particle surface. A color change from red to purple can be induced by the aggregation of the dispersed AuNPs because of the interparticle surface plasmon coupling. Hence, AuNPs-based colorimetric assays often employ functional AuNPs and the change of the aggregation state is induced by target molecules. In a typical assay, AuNPs were formed via cross-linking assembly when targeted molecules existed, thus triggering aggregation of AuNPs and leading to wavelength red shift in the visible region and a red-to-purple change of the solutions. Based on AuNPs aggregation or redispersion induced by the target, colorimetric methods have been developed for the detection of various analytes such as nucleic acids, proteins, metal ions, organic molecules, and pathogens [36–43].

AuNPs have strong surface-plasmon resonance absorption with a high extinction coefficient, which is about four orders of magnitude greater than that of typical organic dyes [10]. Hence, the AuNPs-based colorimetric methods have improved sensitivity compared with conventional colorimetric ELISA in which the color change is induced by organic dyes generated by biocatalysis. The AuNPs-based colorimetric methods are quite simple and useful for many analytes. However, for analytes at the low concentration, such as biomarkers in clinical samples, these methods have insufficient sensitivity and signal amplification approaches are required. To improve the sensitivity, enzyme-based and nucleic acid-based signal amplification reactions were integrated with AuNPs-based colorimetric method [44–47]. For example, a plasmonic ELISA strategy was developed for ultrasensitive biomarker detection and prostate-specific antigen and HIV-1 capsid antigen p24 could be detected at the ultralow concentration of 1×10^{-18} g/mL with naked eyes [44]. Nucleic acid signal amplification reaction is also an effective way to couple conventional methods with AuNPs-based colorimetric method. Kato and *et al*. [47] reported an AuNPs-based DNA assay using enzyme-free click chemical ligation chain reaction (enzyme-free LCR) for signal amplification. In this strategy, target DNA firstly acted as a template to hybridize with the sequences coated on AuNPs and another short DNA sequence, and then click chemical ligation chain reaction occurred between the two captured DNA sequences to form a long sequence which was complementary to the target DNA (Figure 3). In addition, a half target sequence was added to from a full target by click chemical ligation chain reaction. By thermal cycling, the ultrahigh sensitivity for DNA detection (aM levels) was achieved.

In recent years, paper-based microfluidic analytical devices (μPADs) have showed great potential for the development of portable, simple, and inexpensive point-of-care (POC) device. Combining the advantages of AuNPs-based colorimetric methods, various AuNPs-based μPADs have been developed [41–43]. It is envisioned that the AuNPs-based μPADs would be a useful platform for on-site clinic diagnostics and environment mentoring at low cost.

4.2 AuNPs-based fluorescent assay

Fluorescence is a sensitive technique for analyte detec-

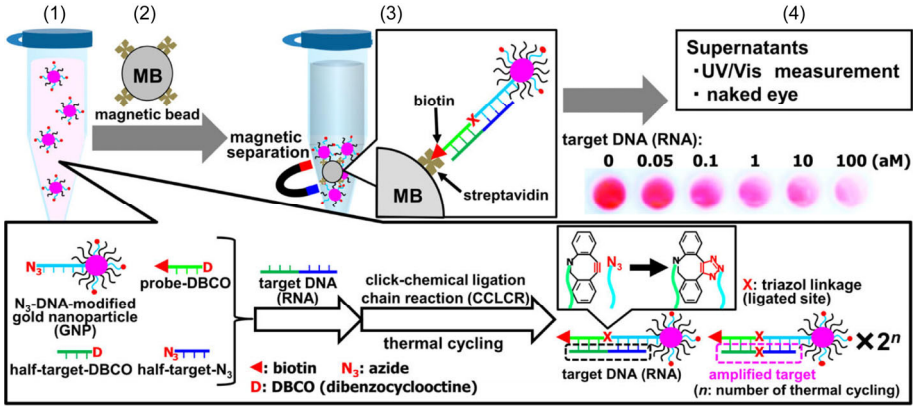

Figure 3 Principles of DNA detection based on click chemical ligation chain reaction. The assay is comprised of four steps: (1) mixture of the N_3-modifed AuNPs, probe-DBCO, and target DNA, and a pair of half-target-N_3 and half-target-DBCO were thermally cycled to amplify exponentially both the biotin-coated AuNPs and the target DNA; (2) addition of streptavidin-coated magnetic beads to capture biotin-coated AuNPs; (3) magnetic separation of the biotin coated AuNPs; (4) using the supernatant for colorimetric detection of DNA target. Reproduced with permission from Ref. [47], Copyright 2014, American Chemical Society (color online).

tion. AuNPs can act as fluorophores and small-sized gold nanoclusters are often employed to this end. The quantum confinement effect of small-sized gold nanoclusters (AuNCs) endows them with enhanced photoluminescence compared to the larger AuNPs [48]. The fluorescence emission wavelength of the AuNCs can be facilely tuned from visible to near-infrared region by controlling the size and chemical composition, thus making them ideal fluorescent nanomaterials for biosensing [49–51]. Various recognition elements such as DNA, protein, peptide, biotin, polymer molecules can be functionalized onto surfaces of AuNCs. The assay often involves the fluorescence quenching by target molecules or self-quenching at the aggregation state of AuNCs induced by target molecules [52–54].

AuNPs can also act as fluorescent quencher in the fluorescent assay. The fluorescence of series fluorophores can be quenched via FRET when they are brought into the close proximity of surface AuNPs due to the extraordinarily high molar extinction coefficients and broad energy bandwidth of AuNPs. A classic detection scheme is based on conformation changes (Figure 4(a)). Fluorophore can be efficiently quenched by AuNPs when it is in the close proximity of the surface of AuNPs. Upon binding with the target molecule, the conformation changes induce fluorophore away from the AuNP, thus allowing fluorescence restoration. This strategy has been widely used to detect DNA, proteins and metal ions [55–57]. Another commonly used strategy is based on the competitive displacement mechanism [58, 59]. Ligands which could bind to the target analyte were conjugated on AuNPs. Then the binding sites of the ligands were blocked by fluorophores-labeled analyte molecules. The fluorescence was quenched by AuNPs. The target molecules in solution could compete with the fluorophore-labeled analytes and restore the fluorescence. The unique optical properties of quantum dots (QD) make them appealing fluorescent labels for biosensing and bioimaging applications [60]. Kim *et al*. [61] developed a method using QDs to replace fluorophore labeled analytes and demonstrated that avidin could be quantitatively detected by the fluorescence recovery of the QDs by using a streptavidin-biotin interaction model system (Figure 4(b)).

AuNPs-based fluorescent assays utilizing the energy transfer between QDs and AuNPs have gained great interest due to the favorable optical properties of QDs [62–64]. In 2015, Uddayasankar *et al*. [64] investigated the impact of the spatial arrangement of the AuNPs and QDs on the analytical performance and demonstrated that multiple QDs around a single AuNP configuration had the better analytical performance. This work provides useful information for the development of sensitive assays utilizing AuNPs and QDs.

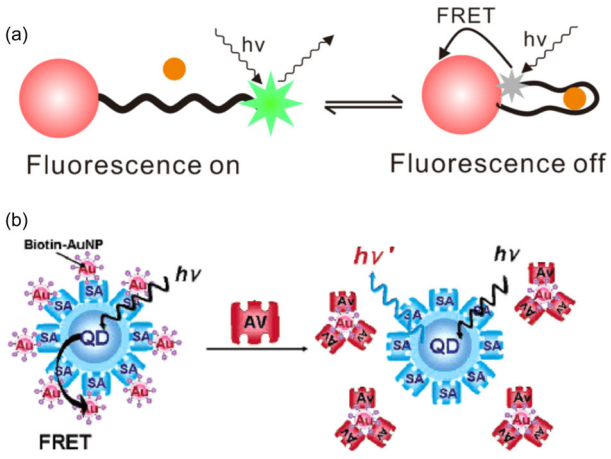

Figure 4 (a) Illustration of fluorescence assay based on conformation change-induced fluorescent "turn on" or "turn off"; (b) demonstration of competitive displacement using QDs. Due to the competitive interaction between streptavidin coated-QDs and target avid with biotin-AuNPs, fluorescent of QDs was restored. Reproduced with permission from Ref. [61], Copyright 2005, American Chemical Society (color online).

4.3 AuNPs-based SERS assay

The Raman spectrum allows detection and identification of analytes since it is sensitive to specific chemical structures. However, the sensitivity of the normal Raman detection is insufficient because the typical Raman signals are quite weak. The magnitude of Raman signal is dramatically enhanced if the Raman-active molecules are close to noble metal surfaces. This effect is termed as surface-enhanced Raman spectroscopy (SERS). AuNPs are good substrates for SERS-based bioassay; the enhanced Raman signal and molecular fingerprint information enable multiplex detection of various analytes with the ultrahigh sensitivity [65–71]. Heterogeneous and homogenous SERS assays are two common detection formats. Heterogeneous SERS assay relies on immobilization of capture probe on a solid surface for capturing target molecules, which can bind with AuNPs functionalized with Raman-labeled probe to form sandwiched structure (Figure 5(A)) [68]. Proteins, DNA, and many other molecules can be detected in this format to achieve the high sensitivity. However, the heterogeneous SERS-based assay is time-consuming and requires several washing steps, which hindered its analytical robustness and reproducibility. Homogenous SERS-based assay is a promising way to achieve robust biosensors. Based on the discovery that SERS signals can be controlled by modulating the electromagnetic field enhancement in the interparticle plasmon coupling, several homogenous SERS-based assays for analytes such as DNA, small ions and proteins have been developed [69–71]. Homogenous SERS assay for protein is a challenge because the large size of antibodies might prevent the closely interacting with AuNPs. A target-controlled assembly-based SERS (TCA-SERS) immunoassay has been developed to achieve orientational immobilization of antibodies for minimization of interparticle distance [69]. This assay employed spherical AuNPs and gold nanorods decorated with half antibody fragments for SERS nanoparticle assembly (Figure 5(B)). The platform has been demonstrated to allow fast, washing-free, and multiplexed quantification of three cytokines (INFγ, IL-2, and TNFα) with the high sensitivity even in complicated biological media. The controlled assembly of SERS nanoparticles is a promising way to achieve tunable, reproducible, and strong plasmonic coupling for biomolecule detection. Exquisite control of nanostructures is important for achieving label-free single-molecule analysis. In 2014, Thacker *et al.* [72] used an innovative DNA origami self-assembly technique to achieve accurate positioning of individual gold nanoparticles. Strong and reproducible plasmonic coupling between two 40-nm gold nanoparticles were observed with gaps less than 5 nm (Figure 5(C)). Several orders of magnitude increased by SERS were observed through the detection of dye molecules and short single-stranded DNA oligonucleotides. Similar work utilizing DNA origami technique for gold nanoparticle assembly and SERS based detection have been reported [72–74]. The novel self-assembly

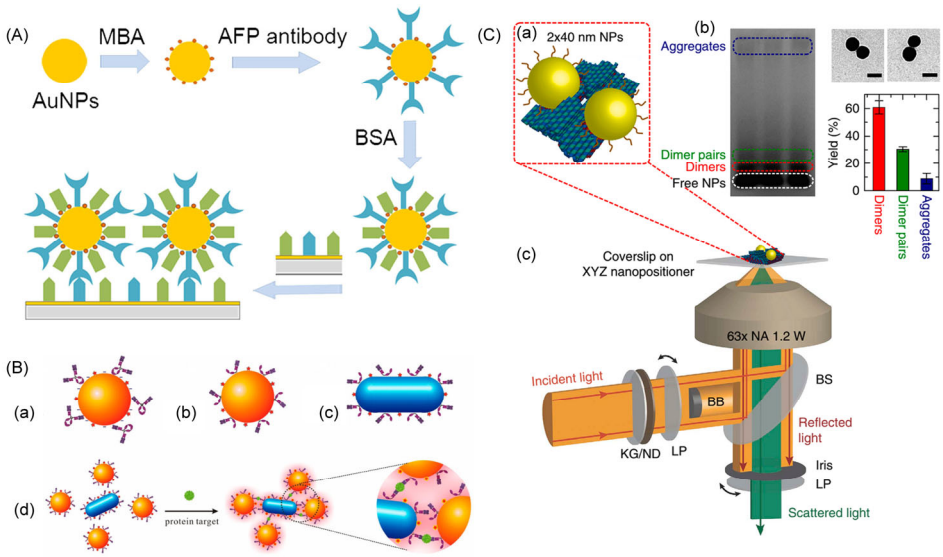

Figure 5 (A) Illustration of Raman reporter-labeled AuNPs preparation and antibody functionalization process (MBA, mercaptobenzoic acid; BSA, bovine serum albumin). (B) Principle of TCA-SERS immunoassay: (a) AuNPs decorated with randomly orientated antibodies via electrostatic assembly for control experiment; (b) AuNPs decorated with orientational antibody half-fragments via Au-thiol assembly; (c) gold nanorods decorated with orientational antibody half-fragments via Au-thiol assembly; (d) single-step SERS immunoassay based on plasmonic coupling enhancement via sandwiched antibody-antigen assembly. (C) (a) Illustration of two gold nanoparticles assembled on the DNA origami platform; (b) gel electrophoresis and TEM characterization of gold nanoparticle dimer; (c) SERS imaging instrument setup (KG, heat absorbing filter; ND, neutral density filter; LP, linear polarizer; BB, beam block; BS, beam splitter). Reproduced with permission from Refs. [68,69,72], Copyright 2013, John Wiley & Sons; and Copyright 2013, American Chemical Society, respectively (color online).

DNA origami technique based on single gold nanoparticles allows formations of various two-dimensional structures and position matter with nanometer accuracy, and provides a reliable and efficient platform for SERS-based application.

5 AuNPs-based cellular imaging

AuNPs possess many desirable properties, which makes them useful for living cell delivery and imaging. The gold core is stable and can be easily functionalized with biomolecules. Various molecules such as nucleic acid, protein, lipid, and peptide can be easily attached to surfaces of AuNPs for targeting cellular biomarkers. The small sizes and tunable surface properties such as surface charges enable fast and effectively penetrating cell membranes into cells. The delivery positions of functionalized AuNPs in cells, such as membrane surface, cytoplasm, organelles or cell nucleus can be devised according to different sizes and shapes of AuNPs and functional biomolecules on the surfaces. The uptake and intracellular fate of AuNPs highly depend on the size, shape, and surface properties of AuNPs [6, 75]. The AuNPs are generally considered to have low cell toxicity. However, investigations of cell toxicity are required for further biological phenomenon study [76–79].

5.1 Fluorescence-based cellular imaging

Fluorescence imaging is now a popular tool for investigating functional molecules and interactions in living cells. One straightforward strategy of utilizing AuNPs for fluorescence imaging is to act as fluorescent labels. To this end, the small-sized gold nanocluster is often employed because the quantum confinement effect of small-sized AuNCs gives them enhanced photoluminescence comparing to larger AuNPs [48]. The fluorescence emission wavelength of the AuNCs can be facilely tuned from visible to near-infrared region by controlling the size and chemical composition, thus making them ideal fluorescent labels. Along with the development of synthesis strategies, AuNCs have been successfully utilized as fluorescence labels for imaging living cells [80–83].

Another imaging strategy is to utilize AuNPs as fluorescence quencher. Since AuNPs have a wide absorption band and strong fluorescence quenching ability, an “off-on” system activated by targets is a useful strategy for imaging and detecting molecules in living cells. In this strategy, fluorescent tags were attached to the surface of AuNPs and was initially quenched; the interaction with target molecules could induce the release of fluorescence tags away from AuNPs surface and restore the fluorescent signal. Mikin’s group [32] utilized the gold core-based SNA construct and developed a “nanoflare” probe for mRNA detection. As shown in Figure 6(a), the nanoflare probe was designed

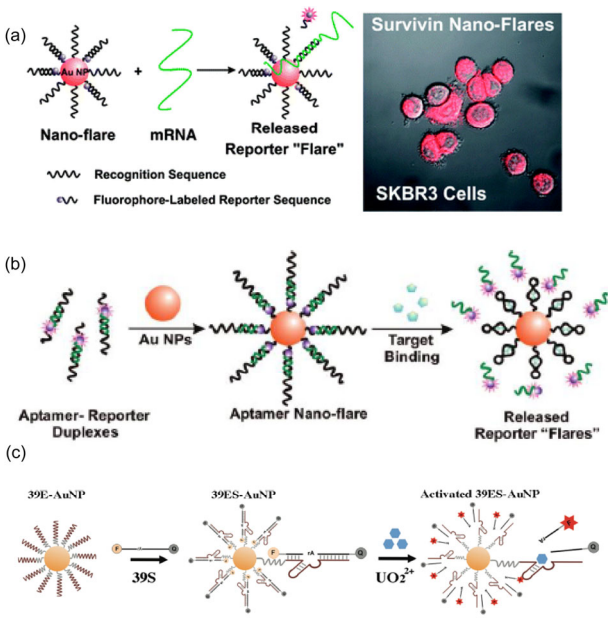

Figure 6 (a) SNA nanoflare functionalized with a recognition sequence of surviving mRNA hybridized with a short complementary fluorophore labeled reporter sequence. Fluorescence “turn on” is achieved upon the fluorophore-labeled reporter sequence leaves from the surface of AuNPs due to the displacement of target mRNA. Survivin mRNA imaging is obtained using survivin-expressing SKBR3 cell treated with SNA nanoflare.. (b) Illustration of aptamer-functionalized SNA construct for target detection based on fluorescence “turn on”. The reporter is displaced by a conformation change of the aptamer induced by the target molecule. (c) Principle of DNAzyme-immobilized AuNPs as a selective probe for detection of uranyl in living cells. Reproduced with permission from Refs. [32,33,85], Copyright 2007, 2009, 2013, American Chemical Society, respectively (color online).

with the strands complementary to target mRNA (~18 bases long) and a fluorophore-labeled “flare” sequence (~10 bases long) was hybridized to the probe. Upon entering cell, the target mRNA was bound with its complementary “nanoflare” probe to displace the short flare sequence from the surface of AuNPs, thus causing an increase in the fluorescence signal. This work was the first time that oligonucleotide-modified AuNPs had been applied for targeting and detecting mRNA in living cells. Multiplexed nanoflares construct was then developed for simultaneously detecting two distinct mRNA targets in living cells [35]. A similar method had been applied to detect mRNA in living cells by employing the molecular beacon construct [84].

The excellent intracellular stability of SNA construct makes it a powerful tool for cellular research because the high local sodium ion concentration around the oligonucleotide is able to deactivate many nucleases [30]. The oligonucleotide-modified AuNPs can be applied for imaging different molecules besides DNA/RNA in living cells utilizing functional DNA probes such as aptamers and DNAzymes. As illustrated in Figure 6(b, c), intracellular ATP and uranyl ion detection were achieved with DNA aptamer-functionalized AuNPs and DNAzyme-AuNPs

probe, respectively [33, 85]. Besides oligonucleotide modification, other biomolecules such as antibody, enzyme, peptide and lipid functionalized AuNPs were also widely used for cellular imaging [34,86–89].

The oligonucleotide-modified AuNPs is a useful platform to deliver nucleic acid reagents and other biomolecules into cells for fluorescence-based imaging of intracellular biomolecules. However, due to the lack of signal amplification, the sensitivity is often limited at the nanomolar level. To improve the detection sensitivity, Wu *et al*. [90] utilized hybridization chain reaction (HCR) to amplify signals for imaging mRNA in living cells. The electrostatic nucleic acid nanoassembly enabled a structure of a gold core, an interlayer of cysteine-terminated cationic peptides, and an outer layer of fluorophore-labeled nucleic acid probes (H1 and H2). The fluorophores were initially quenched by the AuNPs and a chain reaction could be triggered for alternating hybridization between H1 and H2 to produce the long duplex HCR product. Due to the rigid duplex conformation, the HCR product could be dissociated from the surface of AuNPs and bring the two fluorophores into the close proximity, and then foster resonant energy transfer (FRET) between these two fluorophores enabled fluorescent imaging (Figure 7). This signal amplification strategy enabled ultrasensitive imaging of mRNA at the picomolar level and was promising for the low-abundance biomarker discovery.

5.2 Light scattering-based cellular imaging

AuNPs scatter light strongly and light scattering is 4–6 orders of magnitude stronger than the emission of most strongly fluorescent molecules because of the SPR oscillation [10]. The strong light scattered from AuNPs can be detected for imaging by dark field microscopy or similar optical setup [91,92]. As shown in Figure 8, single gold nanoparticle with the diameter of 30–100 nm can be easily detected and the scattering properties (spectra and intensity) highly depend on the size and shapes of AuNPs [93].

Hence, monitoring scattering spectra changes of AuNPs is a useful platform to detect biomolecules and study interaction in living cells because AuNPs are biocompatible and easily functionalized with biomolecules and have the low cell toxicity [94–102]. Ament *et al*. [95] utilized single gold nanorod to detect single protein by monitoring the spectra change from free gold nanorod to protein-bound gold nanorod. Similarly, single mRNA variant detection in living cells has been achieved by monitoring scattering spectral shift from a monomer to dimer gold nanoparticle [96]. Two gold-nanoparticle-conjugated probes were designed to be complementary with the BRCA1 mRNA target and a spectral shift was observed due to dimer formation in the presence of the BRCA1 mRNA target. This approach is able to quantify and differentiate multiple BRCA1 splice variants in living cells with single-copy sensitivity (Figure 9).

Single molecule detection method utilizing scattering spectra changes of individual gold nanoparticle provides a useful platform to study fundamental problems at the molecular level, such as interaction among biomolecules and dynamics of biomolecules in living cells. However, this technique requires relatively large gold nanoparticles and long scanning time to achieve the high signal-to-noise ratio for imaging. Improvements in the optical system development (ie. fast imaging system) will benefit dynamic tracking of single molecule by using individual gold nanoparticles.

5.3 Two-photon photoluminescence-based cellular imaging

Two-photon photoluminescence-based imaging (TPL) is attractive for noninvasive bioimaging in living cells and

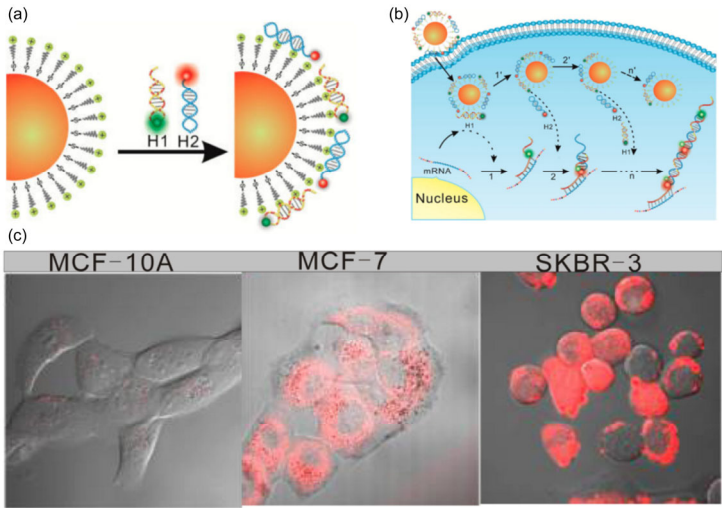

Figure 7 (a) Illustration of the electrostatically assembled DNA nanostructure; (b) intracellular HCR for mRNA detection; (c) fluorescence images for MCF-10A, MCF-7, and SKBR-3 cells incubated with the nanoassembly. Reproduced with permission from Ref. [90], Copyright 2015, American Chemical Society (color online).

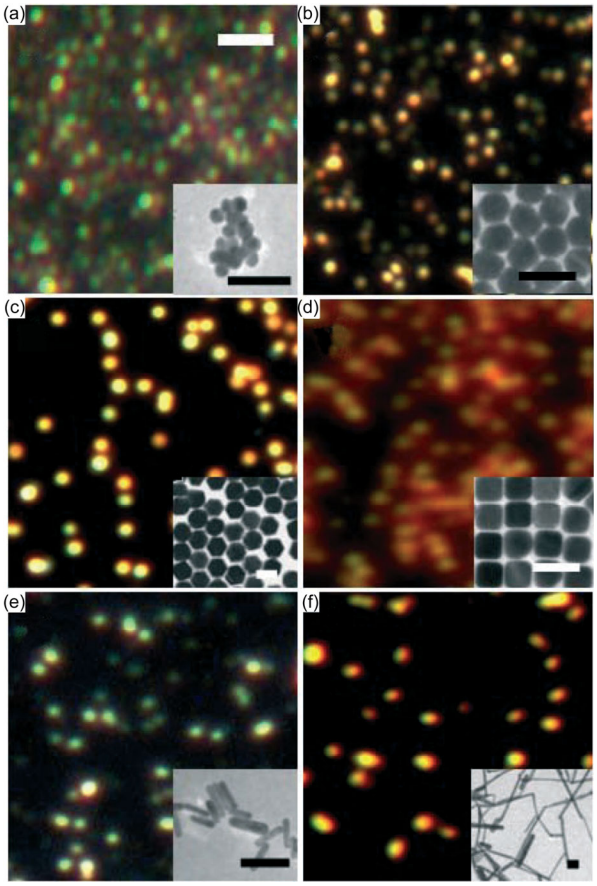

Figure 8 Dark-field light-scattering images of gold nanoparticles and corresponding TEM images. (a) gold nanospheres (diameter =23 nm); (b) gold nanospheres (diameter =70 nm); (c) hexagons; (d) cubes; (e) rods of aspect ratio ≈4.4; (f) nanorods with the aspect ratio ≈16. Scale bars represent 2 μm for dark-field light-scattering images and 100 nm in TEM images. Reproduced with permission from Ref. [93], Copyright 2006, John Wiley & Sons (color online).

tissues due to the unique advantages of this technology, such as the penetration ability into deep tissues, reduced background signal, and low toxicity [103,104]. AuNCs, gold nanorods and AuNPs with different shapes have large two-photon absorption (TPA) cross section than typical organic dyes, the larger or compatible TPA cross section compared with QDs [60,105–108]. AuNPs have the better photostability and biocompatibility and the lower cell toxicity than organic dyes and QDs. All these features make AuNPs a promising material for TPL-based cellular imaging.

The two-photon absorption cross section of AuNPs highly depends on the structure and shape of nanoparticles since the localized surface plasmon resonance (LSPR) is sensitive to shapes. Gao *et al*. [108] investigated the TPL properties of AuNPs of five different shapes (nanospheres, nanocubes, nanotriangles, nanorods, and nanobranches). The TPA cross sections of single nanosphere, nanocube, nanotriangle, nanorod and nanobranch were estimated to be 83, 500, 1.5×10^3, 4.2×10^4, and 4.0×10^6 GM, respectively. Cellular imaging results also demonstrated the better TPL imagines from gold nanobranches-treated cancer cells in contrast to gold nanospheres-treated cancer cells (Figure 10).

The gold nanospheres are not quite suitable for TPL imaging due to the relatively small TPA cross section comparing to that of other shapes of AuNPs. Gold nanorod is a favorable nanostructure for TPL imaging because of the large TPA cross section and single gold nanorod particle is detectable under high signal-to-noise ratio for the small size of 8 nm×40 nm by using two-photon imaging [108,109]. The surface modification of gold nanorod is facile and can only increase the hydrodynamic diameter by several nanometers. Since the size is compatible with complex protein molecules in living cells, TPL utilizing gold nanorods has drawn great interest for studying functional biomolecules in living cells [109–115]. Aside from regular two-dimensional imaging, gold nanorods show the potential for single particle three- dimensional imaging tracking. Van den Broek *et al*. [115] achieved parallel three-dimensional tracking of gold nanorods in live cells by using multifunctional TPL microscopy. Single gold nanorod can be localized with a resolution of 4 nm in the horizontal plane and 8 nm in the vertical direction. This 3D tracking approach is a promising platform for studying biological functions in living cells.

5.4 SERS-based cellular imaging

SERS is a noninvasive detection technique and the Raman fingerprints of individual molecules allow multiplexing imaging because of the narrow width of Raman peaks. Gold nanoparticle is a good substrate for SERS detection because it can improve the Raman signal by several orders of magnitude. Combing the unique advantages of AuNPs for cellular imaging such as the small size, good biocompatibility, and easy functionalization way, AuNPs have been widely used in SERS-based cellular imaging [116, 117]. Kang *et al*. [118] reported a method using three different Raman dyes-coded spherical gold nanoparticles for imaging different locations in living cells. AuNPs were stabilized by oligonucleotides, functionalized with different peptides and Raman reporters, and employed as probes for targeting cytoplasm, mitochondria, and nucleus simultaneously. High-speed and high-resolution living cell Raman images were achieved and allowed to rapidly monitor the changes of cell morphologies. Multiplexed targets, high resolution, and high speed would be good development directions of SERS-based cellular imaging approaches and several progresses were achieved recently [119,120]. It is expected to employ AuNPs as intracellular probes for cellular SERS imaging in biological research such as cancer detection and therapeutics.

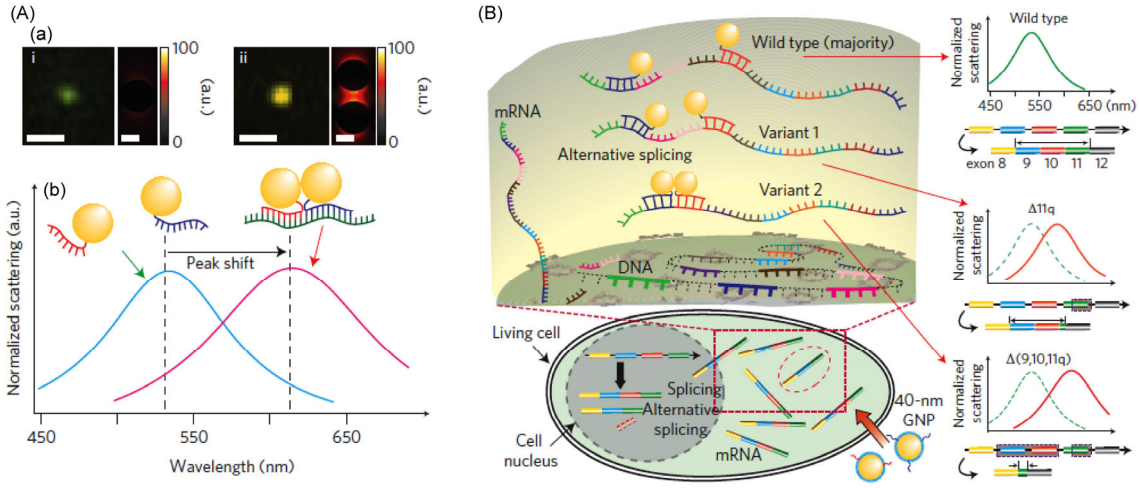

Figure 9 Principles for sequence-specific single mRNA detection. (A) (a) Real-color images and finite-difference time-domain (FDTD) simulation results of the gold nanoparticle monomer and dimer, respectively. Scale bars, 1 mm (real color images) and 20 nm (FDTD simulation results); (b) spectral peak shift induced by DNA hybridization of specific sequence. Monomers (blue line) and dimers (purple line) can be differentiated according to their unique plasmon scattering band. (B) Single mRNA detection in living cells based on spectra change from gold nanoparticle monomer to dimer induced by BRCA1 mRNA. Reproduced with permission from Ref. [96], Copyright 2014, Nature Publishing Group (color online).

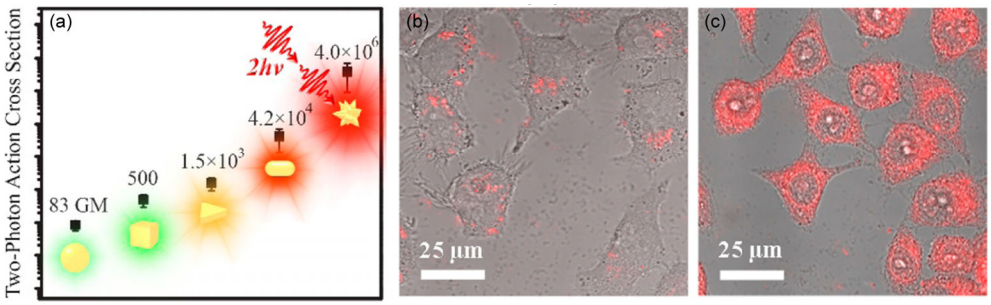

Figure 10 (a) Two-photon absorption cross sections of single gold nanospheres, gold nanocubes, gold nanotriangles, gold nanorods, and gold nanobranches, respectively; (b) TPL image of HepG2 cells after incubation with PVP-modified gold nanospheres; (c) TPL image of HepG2 cells after incubation with PVP-modified gold nanobranches. Reproduced with permission from [108], Copyright 2014, American Chemical Society (color online).

6 Summary and outlook

AuNPs have been widely used in optical biosensing and bioimaging for many kinds of analytes and achieved great successes. The AuNPs can be prepared in facile ways with good reproducibility and surface modification of AuNPs is easy and stable. Sizes, shapes and surface properties of AuNPs can be finely tuned according to different synthesis and functionalization processes. Owing to the enhanced optical properties such as surface plasmon absorption, fluorescence and SERS, analytical performances are improved in sensitivity, selectivity, and speed. However, there are still some issues and challenges to be resolved for practical sample analysis and POC diagnostics. The analytical performances of AuNPs-based biosensors can be improved such as reducing non-specific adsorption to reduce background. Production of AuNPs with long-term stability in various environments should be explored. High-throughput and multiplex detection approaches for large amount of samples utilizing AuNPs are still challenges to be resolved. Hybrids of AuNPs with other nanomaterials may generate distinct optical properties for biosensing. AuNPs integrated with paper-based microfluidic device is a promising way to develop POC diagnostic devices for practical diagnostics.

Due to the excellent biocompatibility, low cell toxicity and optical properties, AuNPs are quite useful for cellular imaging. Signal amplification approaches have been developed to improve the imaging sensitivity of low abundance biomarkers in cells. Based on strong light scattering and two-photon photoluminescence of individual AuNP, single particle tracking and single molecule detection can be achieved in living cells. It is envisioned that AuNPs would play important roles in cellular imaging for studying biological problems. There are some aspects to be explored. Despite the low toxicity, investigation of cell toxicity of AuNPs with different sizes and shapes is still important for further biological study. The development of advanced optical imaging setup such as the fast imaging system will benefit dynamic tracking of individual gold nanoparticle and studies of related biological issues.

Acknowledgments This work was supported by the National Natural Science Foundation of China (Nos. 21527810, 21190041, 21307029, and 21221003).

Conflict of interest The authors declare that they have no conflict of interest.

1 Jiang JH, Tang H. *Encyclopedia Anal Chem*, 2015, doi: 10.1002/9780470027318.a9477
2 Vikesland PJ, Wigginton KR. *Environ Sci Technol*, 2010, 44: 3656–3669
3 Lei JP, Ju HX. *Chem Soc Rev*, 2012, 41: 2122–2134
4 Boisselier E, Astruc D. *Chem Soc Rev*, 2009, 38: 1759–1782
5 Saha K, Agasti SS, Kim C, Li XN, Rotello VM. *Chem Rev*, 2012, 112: 2739–2779
6 Dykman LA, Khlebtsov NG. *Chem Rev*, 2014, 114: 1258–1288
7 Zhou W, Gao X, Liu DB, Chen XY. *Chem Rev*, 2015, 115: 10575–10636
8 Link S, El-Sayed MA. *J Phy Chem B*, 1999, 103: 4212–4217
9 Kelly KL, Coronado E, Zhao LL, Schatz GC. *J Phy Chem B*, 2003, 107: 668–677
10 Jain PK, Lee KS, El-Sayed IH, El-Sayed MA. *J Phy Chem B*, 2006, 110: 7238–7248
11 Njoki PN, Lim IIS, Mott D, Park HY, Khan B, Mishra S, Sujakumar R, Luo J, Zhong CJ. *J Phy Chem C*, 2007, 111: 14664–14669
12 Ringe E, Langille MR, Sohn K, Zhang J, Huang JX, Mirkin CA, Van Duyne RP, Marks LD. *J Phys Chem Lett*, 2012, 3: 1479–1483
13 El-Sayed MA. *Acc Chem Res*, 2001, 34: 257–264
14 Nikoobakht B, El-Sayed MA. *Chem Mater*, 2003, 15: 1957–1962
15 Lee KS, El-Sayed MA. *J Phys Chem B*, 2005, 109: 20331–20338
16 Murphy CJ, Sau TK, Gole AM, Orendorff CJ, Gao J, Gou L, Hunyadi SE, Li T. *J Phys Chem B*, 2005, 109: 13857–13870
17 Chen HJ, Shao L, Li L, Wang JF. *Chem Soc Rev*, 2013, 42: 2679–2724
18 Xia YN, Li WY, Cobley CM, Chen JY, Xia XH, Zhang Q, Yang MX, Cho EC, Brown PK. *Acc Chem Res*, 2011, 44: 914–924
19 Turkevich J, Stevenson PC, Hillier J. *Discuss Faraday Soc*, 1951, 11: 55–75
20 Kimling J, Maier M, Okenve B, Kotaidis V, Ballot H, Plech A. *J Phys Chem B*, 2006, 110: 15700–15707
21 Pérez-Juste J, Pastoriza-Santos I, Liz-Marzán LM, Mulvaney P. *Coord Chem Rev*, 2005, 249: 1870–1901
22 Khoury CG, Vo-Dinh T. *J Phys Chem C*, 2008, 112: 18849–18859
23 Grzelczak M, Pérez-Juste J, Mulvaney P, Liz-Marzán LM. *Chem Soc Rev*, 2008, 37: 1783–1791
24 Zhao PX, Li N, Astruc D. *Coord Chem Rev*, 2013, 257: 638–665
25 Zeng SW, Yong KT, Roy I, Dinh XQ, Yu X, Luan F. *Plasmonics*, 2011, 6: 491–506
26 Torabi SF, Lu Y. *Curr Opin Chem Biol*, 2014, 28: 88–95
27 Brust M, Walker M, Bethell D, Schiffrin DJ, Whyman R. *J Chem Soc Chem Commun*, 1994, 7: 801–802
28 Mirkin CA, Letsinger RL, Mucic RC, Storhoff JJ. *Nature*, 1996, 382: 607–609
29 CutlerJI, Auyeung E, Mirkin CA. *J Am Chem Soc*, 2012, 134: 1376–1391
30 Zwanikken JW, Guo PJ, Mirkin CA, Cruz MO. *J Phys Chem C*, 2011, 115: 16368–16373
31 Rosi NL, Giljohann DA, Thaxton CS, Lytton-Jean AKR, Han MS, Mirkin CA. *Science*, 2006, 312: 1027–1030
32 Seferos DS, Giljohann DA, Hill HD, Prigodich AE, Mirkin CA. *J Am Chem Soc*, 2007, 129: 15477–15479
33 Zheng D, Seferos DS, Giljohann DA, Patel PC, Mirkin CA. *Nano Lett*, 2009, 9: 3258–3261
34 Zhang K, Hao LL, Hurst SJ, Mirkin CA. *J Am Chem Soc*, 2012, 134: 16488–16491
35 Prigodich AE, Randeria PS, Briley WE, Kim NJ, Daniel WL, Giljohann DA, Mirkin CA. *Anal Chem*, 2012, 84: 2062–2066
36 Liu DB, Chen WW, Wei JH, Li XB, Wang Z, Jiang XY. *Anal Chem*, 2012, 84: 4185–4191
37 Wu Z, Wu ZK, Tang H, Tang LJ, Jiang JH. *Anal Chem*, 2013, 85: 4376–4383
38 Sener G, Uzun L, Denizli A. *Anal Chem*, 2014, 86: 514–520
39 Zhang L, Wang ZX, Liang RP, Qiu JD. *Biosens Bioelectron*, 2015, 68: 668–674
40 Soh JH, Lin YY, Rana SU, Ying JY, Stevens MM. *Anal Chem*, 2015, 87: 7644–7652
41 Liang PP, Yu HX, Guntupalli B, Xiao Y. *ACS Appl Mater Interf*, 2015, 7: 15023–15030
42 Choleva TG, Kappi FA, Giokas DL, Vlessidis AG. *Anal Chim Acta*, 2015, 860: 61–69
43 Chen GH, Chen WY, Yen YC, Wang CW, Chang HT, Chen CF. *Anal Chem*, 2014, 86: 6843–6849
44 Rica RD, Stevens MM. *Nat Nanotech*, 2012, 7: 821–824
45 Valentini P, Fiammengo R, Sabella S, Gariboldi M, Maiorano G, Cingolani R, Pompa PP. *ACS Nano*, 2013, 7: 5530–5538
46 Shen W, Deng HM, Gao ZQ. *J Am Chem Soc*, 2012, 134: 14678–14681
47 Kato D, Oishi M. *ACS Nano*, 2014, 8: 9987–9997
48 Jin RC. *Nanoscale*, 2010, 2: 343–362
49 Huang C, Liao H, Shiang Y, Lin Z, Yang Z, Chang H. *J Mater Chem*, 2009, 19: 755–759
50 Pettibone JM, Hudgens JW. *J Phys Chem Lett*, 2010, 1: 2536–2540
51 Xie J, Zheng Y, Ying JY. *J Am Chem Soc*, 2009, 131: 888–889
52 Sun J, Yang F, Zhao D, Yang XR. *Anal Chem*, 2014, 86: 7883–7889
53 Liu JW. *TrAC Trends Anal Chem*, 2014, 58: 99–11
54 Qin L, He XW, Chen LX, Zhang YK. *ACS Appl Mater Interf*, 2015, 7: 5965–5971
55 Dubertret B, Calame M, Libchaber AJ. *Nat Biotech*, 2001, 19: 365–370
56 Luo F, Zheng LY, Chen SS, Cai QY, Lin ZY, Qiu B, Chen GN. *Chem Commun*, 2012, 48: 6387–6389
57 Wang GK, Lu YF, Yan CL, Lu Y. *Sens Actuators B*, 2015, 211: 1–6
58 Wang W, Kong T, Zhang D, Zhang JN, Cheng GS. *Anal Chem*, 2015, 87: 10822–10829
59 Guirgis BSS, Cunha CS, Gomes I, Cavadas M, Silva I, Doria G, Blatch GL, Baptista PV, Pereira E, Azzazy HME, Mota MM, Prudêncio M, Franco R. *Anal Bioanal Chem*, 2012, 402: 1019–1027
60 Resch-Genger U, Grabolle M, Cavaliere-Jaricot S, Nitschke R, Thomas N. *Nat Method*, 2008, 5: 763–775
61 Oh E, Hong MY, Lee D, Nam SH, Yoon HC, Kim HS. *J Am Chem Soc*, 2005, 127: 3270–3271
62 Samanta A, Zhou YD, Zou SL, Yan H, Liu Y. *Nano Lett*, 2014, 14: 5052–5057
63 Huang DW, Niu CG, Wang XY, Lv XX, Zeng GM. *Anal Chem*, 2013, 85: 1164–1170
64 Uddayasankar U, Krull UJ. *Langmuir*, 2015, 31: 8194–8204
65 Sun L, Yu CX, Irudayaraj J. *Anal Chem*, 2007, 79: 3981–3988
66 Lee JH, Nam JM, Jeon KS, Lim DK, Kim H, Kwon S, Lee H, Suh YD. *ACS Nano*, 2012, 6: 9574–9584
67 Porter MD, Lipert RJ, Siperko LM, Wang GF, Narayanan R. *Chem Soc Rev*, 2008, 37: 1001–1011
68 Wang AJ, Ruan WD Song W, Chen L, Zhao B, Jung YM, Wang X. *J Raman Spectrosc*, 2013, 44: 1649–1653
69 Wang Y, Tang LJ, Jiang JH. *Anal Chem*, 2013, 85: 9213–9220
70 Qian XM, Zhou X, Nie SM. *J Am Chem Soc*, 2008, 130: 14934–14935
71 MacAskill A, Crawford D, Graham D, Faulds K. *Anal Chem*, 2009, 81: 8134–8140
72 Thacker VV, Herrmann LO, Sigle DO, Zhang T, Liedl T, Baumberg JJ, Keyser UF. *Nat Commun*, 2014, 5: 3448
73 Kühler P, Roller EM, Schreiber R, Liedl T, Lohmüller T, Feldmann J. *Nano Lett*, 2014, 14: 2914–2919
74 Pilo-Pais M, Watson A, Demers S, LaBean TH, Finkelstein G. *Nano Lett*, 2014, 14: 2099–2104
75 Yao MF, He LL, McClements DJ, Xiao H. *J Agric Food Chem*, 2015, 63: 8044–8049
76 Lewinski N, Colvin V, Drezek R. *Small*, 2008, 4: 26–49
77 Boisselier E, Astruc D. *Chem Soc Rev*, 2009, 38: 1759–1782

78 Khlebtsov N, Dykman LA. *Chem Soc Rev*, 2011, 40: 1647–1671
79 Murphy CJ, Gole AM, Stone JW, Sisco PN, Alkilany AM, Goldsmith EC, Baxter SC. *Acc Chem Res*, 2008, 41: 1721–1730
80 Han YY, Ding CQ, Zhou J, Tian Y. *Anal Chem*, 2015, 87: 5333–5339
81 Liu JM, Chen JT, Yan XP. *Anal Chem*, 2013, 85: 3238–3245
82 Lin SY, Chen NT, Sum SP, Lo LW, Yang CS. *Chem Commun*, 2008, 39: 4762–4764
83 Zhang CL, Li C, Liu YL, Zhang JP, Bao CC, Liang SJ, Wang Q, Yang Yao, Fu HL, Wang K, Cui DX. *Adv Funct Mater*, 2015, 25: 1314–1325
84 Jayagopal A, Halfpenny KC, Perez JW, Wright DW. *J Am Chem Soc*, 2010, 132: 9789–9796
85 Wu PW, Hwang K, Lan T, Lu Y. *J Am Chem Soc*, 2013, 135: 5254–5257
86 Ghosh P, Yang XC, Arvizo R, Zhu ZJ, Agasti SS, Mo ZH, Rotello VM. *J Am Chem Soc*, 2010, 132: 2642–2645
87 Lu H, Wang DL, Kazane S, Javahishvili T, Tian F, Song F, Sellers A, Barnett B, Schultz PG. *J Am Chem Soc*, 2013, 135: 13885–13891
88 Banga RJ, Chernyak N, Narayan SP, Nguyen ST, Mirkin CA. *J Am Chem Soc*, 2014, 136: 9866–9869
89 Elmes RBP, Orange KN, Cloonan SM, Williams DC, Gunnlaugsson T. *J Am Chem Soc*, 2011, 133: 15862–15865
90 Wu Z, Liu GQ, Yang XL, Jiang JH. *J Am Chem Soc*, 2015, 137: 6829–6836
91 Liu MM, Chao J, Deng SH, Wang K, Li K, Fan CH. *Coll Surf B*, 2014, 124: 111–117
92 Jin HY, Li DW, Zhang N, Gu Z, Long YT. *ACS Appl Mater Interf*, 2015, 7: 12249–12253
93 Orendorff CJ, Sau TK, Murphy CJ. *Small*, 2006, 2: 636–639
94 Aioub M, Kang B, Mackey MA, El-Sayed MA. *J Phys Chem Lett*, 2014, 5: 2555–2561
95 Ament I, Prasad J, Henkel A, Schmachtel S, Sonnichsen C. *Nano Lett*, 2012, 12: 1092–1095
96 Lee1 K, Cui Y, Lee1 LP, Irudayaraj J. *Nat Nanotech*, 2014, 9: 474–480
97 Fairbairn N, Christofidou A, Kanaras AG, Newman TA, Muskens OL. *Phys Chem Chem Phys*, 2013, 15: 4163–4168
98 Liu H, Dong CQ, Ren JC. *J Am Chem Soc*, 2014, 136: 2775–2785
99 Zijlstra P, Paulo PMR, Orrit M. *Nat Nanotech*, 2012, 7: 379–382
100 Wan XY, Zheng LL, Gao PF, Yang XX, Li CM, Li YF, Huang CZ. *Sci Rep*, 2014, 4: 4529–4536
101 Xu D, He Y, Yeung ES. *Anal Chem*, 2014, 86: 3397–3404
102 Piliarik M, Sandoghdar V. *Nat Commun*, 2014, 5: 4495
103 So PTC, Dong CY, Masters BR, Berland KM. *Annu Rev Biomed Eng*, 2000, 2: 399–429
104 Svoboda K, Yasuda R. *Neuron*, 2006, 50: 823–839
105 Larson DR, Zipfel WR, Williams RM, Clark SW, Bruchez MP, Wise FW, Webb WW. *Science*, 2003, 300: 1434–1436
106 Liu CL, Ho ML, Chen YC, Hsieh CC, Lin YC, Wang YH, Yang MJ, Duan HS, Chen BS, Lee JF, Hsiao JK, Chou PT. *J Phys Chem C*, 2009, 113: 21082–21089
107 Polavarapu L, Manna M, Xu QH. *Nanoscale*, 2011, 3: 429–434
108 Gao NY, Chen Y, Li L, Guan ZP, Zhao TT, Zhou N, Yuan PY, Yao SQ, Xu QH. *J Phys Chem C*, 2014, 118: 13904–13911
109 Wang HF, Huff TB, Zweifel DA, He W, Low PS, Wei A, Cheng JX. *Proc Natl Acad Sci USA*, 2005, 122: 15752–15756
110 Verellen N, Denkova D, Clercq BD, Silhanek AV, Ameloot M, Dorpe P, Moshchalkov VV. *ACS Photonic*, 2015, 2: 410–416
111 Durr NJ, Larson T, Smith DK, Korgel BA, Sokolov K, Ben-Yakar A. *Nano Lett*, 2007, 7: 941–945
112 Jiang XF, Pan YL, Jiang CF, Zhao TT, Yuan PY, Venkatesan T, Xu QH. *J Phys Chem Lett*, 2013, 4: 1634–1638
113 Guan ZP, Gao NY, Jiang XF, Yuan PY, Han F, Xu QH. *J Am Chem Soc*, 2013, 135: 7272–7277
114 Zhao TT, Yu K, Li L, Zhang TS, Guan ZP, Gao NY, Yuan PY, Li S, Yao SQ, Xu QH, Xu GQ. *ACS Appl Mater Interf*, 2014, 6: 2700–2708
115 Van den Broek B, Ashcroft B, Oosterkamp TH, van Noort J. *Nano Lett*, 2013, 13: 980–986
116 Vendrell M, Maiti KK, Dhaliwal K, Chang YT. *Trends Biotechnol*, 2013, 31: 249–257
117 Kneipp J, Kneipp H, Wittig B, Kneipp K. *Nanomed Nanotech Biol Med*, 2010, 6: 214–226
118 Kang JK, So PTC, Dasari RR, Lim DK. *Nano Lett*, 2015, 15: 1766–1772
119 Panikkanvalappil SR, Hira SM, Mahmoud MA, El-Sayed MA. *J Am Chem Soc*, 2014, 136: 15961–15968
120 Huefner A, Kuan WL, Barker RA, Mahajan S. *Nano Lett*, 2013, 13: 2463–2470